Title: The anti-IgE mAb Omalizumab induces adverse reactions by engaging Fcγ receptors

Authors

Bianca Balbino[1,2], Pauline Herviou[1], Ophélie Godon[1], Julien Stackowicz[1,2], Odile Richard-Le Goff[1], Bruno Iannascoli[1], Delphine Sterlin[1,3], Sébastien Brûlé[4], Gael A. Millot[5], Faith M. Harris[6], Vera A. Voronina[6], Kari C. Nadeau[7,8], Lynn E. Macdonald[6], Andrew J. Murphy[6], Pierre Bruhns[1,*] and Laurent L. Reber[1,9,*]

Affiliations

[1]Unit of Antibodies in Therapy and Pathology, Institut Pasteur, UMR1222 INSERM, F-75015 Paris, France. [2]Sorbonne Université, Paris, France. [3]Assistance Publique–Hôpitaux de Paris (AP-HP), La Pitié-Salpêtrière, Département d'Immunologie, France, Paris. [4]Plateforme de biophysique moléculaire, Institut Pasteur, UMR 3528 CNRS, Paris 75015, France. [5]Hub de Bioinformatique et Biostatistique – Département Biologie Computationnelle, Institut Pasteur, USR 3756 CNRS, Paris, France. [6]Regeneron Pharmaceuticals Inc., Tarrytown, NY 10591, USA. [7]Sean N. Parker Center for Allergy and Asthma Research, Stanford University, Stanford, California, USA. [8]Division of Pulmonary and Critical Care, Department of Medicine, Stanford University, California, USA. [9]Center for Physiopathology of Toulouse-Purpan (CPTP), UMR 1043, University of Toulouse, INSERM, CNRS, Toulouse, France. [*]These authors contributed equally to this work.

Corresponding authors

Laurent L. Reber, Ph.D

ATIP-Avenir team "Asthma, Allergy & Immunotherapy"

Center for Physiopathology Toulouse-Purpan (CPTP)

CHU Purpan – BP 3028

31024 Toulouse Cedex 3, France

Phone: +33-5-6274-4529

e-mail: laurent.reber@inserm.fr

Pierre Bruhns, Ph.D.

Unit of Antibodies in Therapy and Pathology

Department of Immunology

Institut Pasteur

25 rue du Docteur Roux

Paris, 75015, France

Phone: +33-1-4568-8629

e-mail: bruhns@pasteur.fr

Running title

Xolair induces FcγR-dependent inflammation

Supplemental methods

Mice. hFcγR^{KI} and FcγR^{null} mice were generated by Regeneron Pharmaceuticals Inc. to express hFcγRI, hFcγRIIa$_{H131}$, hFcγRIIb$_{I232}$, hFcγRIIc$_{stop13}$, hFcγRIIIa$_{V158}$ and hFcγRIIIb$_{NA2}$ polymorphic variants, or no FcγR, respectively, as described previously (1). hFcRn^{KI} (VG1481) and hβ2m^{KI} (VG5153) mice were designed and generated by Regeneron Pharmaceuticals Inc (see Figure S5 for the genomic coordinates). Construction of the long targeting vectors and targeting of ES cells was performed as previously described (2). To generate C1q$^{-/-}$ (VG598) mice, the mouse C1qA, C1qB, and C1qC genes were deleted and a LacZ gene was inserted under control of the mouse C1qA promotor. Genomic coordinates for the deletion are Chr4:136,880,289-136,897,837 based on a mouse (GRCm38.p4) genomic assembly. hFcγR^{KI}hFcRn^{KI}hβ2m^{KI} mice were generated by intercrossing of hFcγR^{KI} mice with both hFcRn^{KI} (VG1481) and hβ2m^{KI} (VG5153) designed and generated by Regeneron Pharmaceuticals Inc. on a mixed 62.5% C57BL/6N and 37.5% 129S6/SvEv genetic background. hFcγR^{KI}C1q$^{-/-}$ mice were generated by intercrossing hFcγR^{KI} mice with C1q$^{-/-}$ mice. hFcεRI^{Tg} mice were described previously (3). Nude-hFcγR^{KI} and nude-hFcγR^{null} mice were obtained by intercrossing NMRI-Foxn1$^{nu/nu}$ (nude) (Janvier labs) mice with hFcγR^{KI} and FcγR^{null} mice, respectively. mFcγR^{null}hFcγRIIA^{tg} mice were described previously (1). All mice were bred at Institut Pasteur and demonstrated normal development and breeding patterns. We used sex and age-matched mice for all experiments.

In vitro formation of Omalizumab/IgE immune complexes (ICs). All antibodies were centrifuged at 13.000 *g* for 15 min to remove any possible aggregate in stock solution. ICs were formed by incubating anti-NP IgE or FITC-labelled anti-NP IgE with Omalizumab or Fc-engineered anti-IgE mAbs at a 1:2 ratio for 1 h at 37°C under agitation (250 rpm).

Binding of ICs to FcγRs expressed on CHO cells. We use a collection of Chinese Hamster Ovarian (CHO) transfectants expressing FLAG-tagged human FcγRs (4) to assess binding of preformed ICs to various FcγRs. Briefly, preformed ICs made of FITC-labelled IgE and Omalizumab or Fc-engineered anti-IgE mAbs were incubated with $5x10^4$ CHO transfectants for 1 h on ice. Cells were washed with MACS buffer (PBS/0.5% BSA/ 2mM EDTA). Cell-bound ICs were detected using MACSQuant flow cytometer (Miltenyi Biotec), and data were analyzed using Flowjo Software (Tree Star). CHO transfectants incubated with FITC-labelled IgE alone were used as a negative control. Expression of human FcγR on the surface of each CHO transfectant was confirmed by flow cytometry using antibodies against FcγRI (10.1), FcγRIIA/IIB (AT.10) and FcγRIIIA/IIIB (MEM-154), all from BD Biosciences.

IC-mediated activation of neutrophils. EDTA-collected blood from healthy donors was obtained from the blood bank ("Etablissement Français du Sang" EFS). Human neutrophils were purified with MACSxpress Neutrophil Isolation Kit (Miltenyi) according to the manufacturer's instructions, and neutrophils purity was assessed by flow cytometry (human neutrophils were defined as $CD45^+CD15^+CD66^+$ cells). Purified human neutrophils were kept in RPMI medium containing 10% FCS, 10 ng/ml clinical-grade G-

CSF (Miltenyi) and 50 ng/ml recombinant human IFN-γ (Miltenyi) at $5x10^5$ cells/ml. Mouse neutrophils were purified from the tibia and femur of $hFc\gamma R^{KI}$ and $Fc\gamma R^{null}$ mice by negative selection using the EasySep Mouse Neutrophil Enrichment kit (STEMCELL Technologies; >90% $Ly6G^+$ $CD11b^+$ on average) according to the manufacturer's instructions, and neutrophils purity was assessed by flow cytometry (mouse neutrophils were defined as $CD45^+CD11b^+Ly6G^+$ cells). Purified mouse neutrophils were primed in RPMI medium containing 10% FCS, 10 ng/ml mouse M-CSF (Miltenyi) and 50 ng/ml mouse IFN-γ (Miltenyi) at $5x10^5$ cells/ml for 16 h before activation with ICs. Activation of human or mouse neutrophils by ICs was performed as previously described (5). Briefly, immobilized ICs were formed by coating 96-well plates (Costar) with IgE (50 μg/ml) in 50 mM carbonate/bicarbonate buffer (pH 9.6) for 16 h, followed by blocking with 10% Ultra Low IgG FBS (Invitrogen) in PBS for 2 h and an incubation with Omalizumab or Fc-engineered anti-IgE mAbs at 100 μg/ml for 1 h in PBST (PBS 0.05% Tween20). Plates were washed 3 times with PBS, and purified neutrophils were incubated at $5x10^4$ cells/well for 1 h at 37°C. Human neutrophils were stained with fluorescently-labeled anti-CD45, anti-CD15, anti-CD66 and anti-CD62L antibodies (all from Miltenyi) for 30 min at 4°C. Mouse neutrophils were stained with fluorescently-labeled anti-CD45, anti-CD11b, anti-Ly6G and anti-CD62L antibodies (all from BD Pharmigen) for 30 min at 4°C. Activation of mouse or human neutrophils was assessed by measuring changes in expression of CD62L. Data were acquired using a MACSQuant flow cytometer (Miltenyi), and analyzed with Flowjo Software (Tree Star). Dead cells (identified by staining with propidium iodide; Gibco) were not included in the analysis.

ICs-induced skin inflammation and myeloperoxidase (MPO) activity. Pre-formed ICs were diluted in saline and injected subcutaneously (s.c.) in the back skin of nude-hFcγR^{KI} or nude-hFcR^{null} mice at a final concentration of 100 μg IgE and 200 μg anti-IgE IgG1 mAbs in 50 μL. We injected saline, IgE or anti-IgE alone (diluted in the same conditions) as a control. Bioluminescent imaging of MPO activity was used as a readout of skin inflammation 2 h after ICs injection as described previously (6, 7). Briefly, mice were injected intraperitoneally (i.p.) with luminol (Sigma; 200 mg/kg in 100 μL). 10 min later, bioluminescence resulting from MPO-mediated oxidation of luminol (3) was imaged using an IVIS Spectrum (PerkinElmer) with 5 min acquisition time using an open filter and medium binning. Total photon flux (photons/seconds) was calculated using Living-Image-v4.5 software (Xenogen Product from PerkinElmer).

ICs-mediated passive systemic anaphylaxis (PSA). Pre-formed ICs were diluted in saline and injected i.v. in hFcγR^{KI}, FcγR^{null} mice at a final concentration of 250 μg IgE and 500 μg anti-IgE in 100μL to induce anaphylaxis. We injected saline, IgE or anti-IgE alone (diluted in the same conditions) as a control. For experiments involving hFcγR^{KI}C1q$^{-/-}$ mice, PSA were performed using pre-formed ICs at the final concentration of 500 μg IgE and 1000 μg anti-IgE in 100μl diluted in saline. Blocking of hFcγRIII was achieved by intravenous injection of 200 μg per mouse of blocking anti-hFcγRIII (clone 3G8) or isotype control (IgG1) 6 hours before ICs injection. Rectal temperature measurements were performed using a digital thermometer (YSI) immediately before (time 0) and at different time points for up to 1 h after injection of ICs.

Human IgE-mediated passive systemic anaphylaxis . hFcεRI^{Tg} mice were injected intravenously (i.v.) with 700 μg anti-IgE IgG1 (Omalizumab or Fc-engineered anti-IgE mAbs) in 100 μL saline, or saline only as a control. 30 min later, mice were sensitized i.v. with 10 μg anti-NP IgE. 16 h later, mice were challenged i.v. with 500 μg NP-BSA (ratio: >20 NP molecules per BSA molecule) (Santa Cruz). Rectal temperature measurements were performed using a digital thermometer (YSI) immediately before (time 0) and at different time points for up to 1 h after challenge with NP.

Omalizumab. Omalizumab (Novartis/Genentech) was dialyzed with PBS for all *in vitro* and *in vivo* experiments.

Cloning and production of WT and Fc-engineered anti-IgE mAbs. Publicly available Omalizumab V_H and V_L sequences (https://www.drugbank.ca/drugs/DB00043) were reverse transcribed into DNA and codon optimized for expression in human cells using IMGT-V-Quest software. V_H and V_L DNA fragments were synthesized by Eurofins. The Omalizumab V_H sequence was cloned into a human pUC19-Igγ1-expressing vector (a kind gift from Hugo Mouquet, Institut Pasteur, Paris) using SalI and AgeI restriction sites, and Omalizumab V_L sequence was cloned into human Igκ-expressing vector using AgeI and BsiWI restriction sites, as previously described (8). For Fc-engineered mAbs, point mutations in the Igγ1-expressing vector were introduced at position 297 (N297A, thereafter named 'NA' mutant) using the QuickChange Site-Directed Mutagenesis Kit (Agilent Technologies), according to the manufacturer's instructions. All vectors were sequenced before being used for antibody production. Antibodies were produced by transient co-

159 transfection of WT or Fc-engineered V_H and V_L expression plasmids into exponentially
160 growing Freestyle™ HEK 293-F (Thermo Fisher Scientific) that were cultured in serum-
161 free Freestyle™ 293 Expression Medium (Life Technologies) in suspension at 37°C in a
162 humidified 8% CO_2 incubator on a shaker platform rotating at 110 rpm. Twenty-four hours
163 before transfection, cells were harvested by centrifugation at 300 *g* for 5 min and
164 resuspended in Freestyle™ 293 Expression Medium at a density of 1 x 10^6 cells/ml, and
165 cultured overnight in the same conditions as mentioned above. For the production of mAbs,
166 40 µg of V_H and V_L expressing plasmids were diluted in 80 µl of FectoPRO reagent
167 (PolyPlus) at a final DNA concentration of 0.8 µg/ml, incubated for 10 minutes at RT
168 before addition to the cells. Twenty-four hours post-transfection, cells were diluted 1:1
169 with Freestyle™ 293 Expression Medium. Cells were cultured for 6 days after transfection.
170 Supernatants were harvested, centrifuged at 4200 rpm for 30 min and filtered (0.2 µm).
171 Antibodies were purified by affinity chromatography using an AKTA pure FPLC
172 instrument (GE Healthcare) and HiTrap Protein G Column (GE Healthcare). After
173 purification, mAbs were desalted with HiTrap Desalting Column (GE Healthcare).
174
175 ***Production of human IgE antibodies***. JW8/5/13 (ECACC 87080706) cells were obtained
176 from Sigma-Aldrich. This cell line produces a chimeric human IgE antibody directed
177 against the hapten 4-hydroxy-3-nitrophenacetyl (NP), and composed of the human Fc ε
178 chain and mouse anti-NP variable chain (we refer to this antibody as 'human IgE' in the
179 manuscript). JW8/5/13 cells were cultured in complete Dulbecco-modified Eagle medium
180 (DMEM, Gibco) containing 2 mM glutamine (Thermo Fisher Scientific) and 10% Foetal
181 Bovine Serum (FBS) (Thermo Fisher Scientific) at 9x10^5 cells/ml. After 15 days,

supernatants were harvested, centrifuged at 4200 rpm for 30 min and filtered (0.2 μm). We purified IgE antibodies by affinity chromatography. Briefly, CNBr-activated Sepharose 4 Fast Flow Beads (GE Healthcare) were coupled with WT anti-IgE using a ratio of 2.5 mg of protein for each gram of beads. Beads were weighted, washed with 15 volumes of cold 1mM HCl and centrifuged for 5 min at 2500 rpm. WT anti-IgE were resuspended in coupling solution (0.1 M $NaHCO_3$ pH 8.3 containing 0.5M NaCl) and mixed with beads overnight at 4°C under agitation. Beads were washed with coupling buffer and non-reacted groups were blocked with 0.1 M Tris-HCl buffer pH 8.0. WT anti-IgE-coupled beads were then washed using alternate low (0.1 M acetate buffer pH 3) and high (0.1 M Tris-HCl pH 8) pH solutions and stored in Borate buffer (100 mM Borate, 150 mM NaCl pH 8.0) at 4°C until use. For purification of IgE, WT anti-IgE-coupled sepharose beads were packed in XK 16/20 Column (GE Healthcare) and affinity chromatography was performed using an AKTA pure FPLC instrument (GE Healthcare). After purification, IgE antibodies were desalted with HiTrap Desalting Column (GE Healthcare), and stored at 4°C until use. For some experiments, purified IgE antibodies were conjugated with FITC using the Pierce Antibody labeling kit (Thermo Fisher Scientific) according to the manufacturer's instructions.

Molecular mass measurements. Antibodies and complexes were analyzed by size exclusion chromatography (SEC) coupled with on-line static light scattering (SLS) system. Prior to equilibration of buffer and injection of protein samples, solutions were passed through 0.2 μm filters. Samples were separated on a Superose 6 Increase 10/300 GL column (GE Healthcare) in Dulbecco's phosphate-buffered saline at 18°C. Samples were

run at 0.7 mg/mL through the gel filtration column with a constant flow at 0.3 ml/min controlled by a GPCmax module. Column was coupled to a triple detector array (TDA) model 302 (Malvern Panalytical, UK) with a static light scattering cell (7 and 90°), a deflection refractometer, a photometer and a differential viscometer. Calibration was done on bovine serum albumin (Sigma) with an injection of 200 µL at 2 mg/mL. Data were recorded and processed using the Omnisec software (Malvern Panalytical, UK).

Binding of Omalizumab or Fc-engineered anti-IgE mAbs to human C1q. To measure binding of Omalizumab or Fc-engineered anti-IgE mAbs to human C1q, 96-well plates (Costar) were coated with increasing concentrations of each mAb (12.5 to 200 ng/well) in 50 nM carbonate-bicarbonate buffer (pH 9.6) at 4°C for 16 h. Plates were washed 3 times with PBS containing 0.05% Tween 20 (PBST) (Sigma-Aldrich), and blocked for 2 h at room temperature in PBST containing 0.1% gelatine and 3% Bovine Serum Albumin (BSA - Roche). Plates were washed 3 times before addition of native human C1q (Abd Serotec) at 1 ng/µL. After 16 h, plates were washed with PBST and incubated 1 h with 50 µL of PBS containing 1 µg/mL anti-human C1q HRP (Abd Serotec). Plates were washed 3 times with PBST before addition of 100 µL/well OPD peroxidase (Sigma). The reaction was stopped by addition of 50 µL 2M H_2SO_4 and absorbance was recorded at 492 nm and corrected at 620 nm.

Binding of Omalizumab or Fc-engineered anti-IgE mAbs to human IgE. To measure binding of Omalizumab or Fc-engineered anti-IgE mAbs to human IgE, 96-well plates (Costar) were coated with each mAb (0.5 µg/well) in 50 nM carbonate-bicarbonate buffer

(pH 9.6) at 4°C for 16 h. Plates were washed 3 times with PBST, and blocked for 2 h at room temperature in PBST 1% BSA. Plates were washed 3 times before addition of increasing doses of IgE (1.6 to 5000 ng/well). After 3 hours, plates were washed with PBST and incubated with 1:10.000 of anti-human IgE (Bethyl) for 1 h. Plates were washed 3 times with PBST before addition of 100 µL/well OPD peroxidase (Sigma). The reaction was stopped by addition of 50 µL 2M H_2SO_4 and absorbance was recorded at 492 nm and corrected at 620 nm.

***Detection of mouse and human FcRn and β2m* transcripts**: Total RNA was extracted from human peripheral blood mononuclear cells or murine splenocytes using NucleoSpin RNA plus kit (Macherey-Nagel) according to the manufacturer's instructions. cDNA were generated at 50°C for 60 minutes using random primers and SuperScript III Reverse Transcriptase (Invitrogen). The primer pairs for FcRn gene (human: 5'-CTCTCCCTCCTGTACCACCTT-3'; 5'-ATAGCAGGAAGGTGAGCTCCT-3'; mouse : 5'-AGCTCAAGTTCCGATTCCTG-3'; 5'- GATCTGGCTGATGAATCTAGGTC-3') and for β2-microglobulin gene (human : 5'-GGCTATCCAGCGTACTCCAAA-3' ; 5'-CGGCAGGCATACTCATCTTTT-3' ; mouse : 5'- CCGGAGAATGGGAAGC -3 ; 5'-GTAGACGGTCTTGGGC -3') were used for amplification with GoTaq G2 polymerase (Promega). Amplification was performed by 35 cycles PCR each consisting of 94°C for 1 min, 58°C for 1 min, 72°C for 1 min. At the end of the 35 cycles, samples were run for an additional 10 min at 72°C and analyzed by 1.5% agarose gel electrophoresis. The expected size of the PCR products: Human FcRn: 450bp; Mouse FcRn: 240 bp; Human β2m: 240 bp; Mouse β2m: 270 bp.

Recirculation of Fc-engineered anti-IgE antibodies in vivo. hFcγR^{KI}hFcRn^{KI}hβ2m^{KI} mice were injected i.p. with 100 μg of Omalizumab, WT or NA anti-IgE mAbs in 100 μL 0.9% NaCl solution. Serum was then collected every 7 or 14 days starting from day 1 post-injection and stored at -20°C until use. Serum levels of anti-IgE mAbs were quantified by ELISA. Briefly, 96-well plates (Costar) were coated with F(ab')2 Goat Anti-human IgG (5μg/mL; Jackson ImmunoResearch) in 50 nM carbonate-bicarbonate buffer (pH 9.6) at 4°C for 16 h. Plates were washed 3 times with PBST, and blocked for 2 h at room temperature in PBST containing 1% BSA. Plates were washed 3 times before addition of serial dilutions of serum (1/100 to 1/3000). After 3 hours, plates were washed with PBST and incubated with goat anti-human kappa HRP (1:4.000; Southern Biotech) for 1 h. Plates were washed 3 times with PBST before addition of 100 μL/well OPD peroxidase (Sigma). The reaction was stopped by addition of 50 μL 2M H_2SO_4 and absorbance was recorded at 492 nm and corrected at 620 nm.

Generation of peripheral blood derived-cultured human mast cells (hMCs). hMCs were generated as described previously (9). Briefly, peripheral blood mononuclear cells were separated using Ficoll-Paque PLUS (GE Healthcare) and CD34$^+$ cells were isolated with a human CD34 positive selection kit (StemCell Technologies). Cells were seeded at 1x10^6 cells/mL in StemSpan medium (StemCell Technologies) supplemented with Ciprofloxacin (10 μg/ml; Sigma-Aldrich), recombinant human IL-6 (50 ng/ml; Peprotech), human IL-3 (50 ng/ml; Peprotech) and SCF (100 ng/mL; Miltenyi). Every three to four days, cultures were doubled in volume with fresh supplemented medium for 30 days. Cells were then

progressively transferred to Iscove's-modified Dulbecco's medium (IMDM; Gibco) supplemented with 50 μM 2-mercaptoethanol (Life Technologies), 0.5% BSA, 1% Insulin-Transferrin-Selenium (Life Technologies), Ciprofloxacin (10 ug/ml), human IL-6 (50ng/mL) and human SCF (100 ng/mL). hMCs were supplemented with fresh medium every week. All data presented were generated with cells after 10 weeks of culture, and co-expression of FcεRI and CD117 was verified by flow cytometry.

Statistical analyses. The R environment was used for all the analyses (10). Data were neither averaged nor normalized prior analyses. When required and when possible, explained variables were log2 converted for better adjustment to linear models. Data were fitted to a linear model that include all the variables plus their interactions, except the technical replicate variable for which variation was left in the residual error. Explanatory quantitative variables (time points, concentration points, etc.) were considered as qualitative to overcome the violation of ancova assumptions. Mixed models were used in case of nested experiment designs using the lmer function of the lme4 package. ANOVA analyses were performed with the Anova function of the car package. Type 3 Sum of Squares was applied on unbalanced designs. In the presence of aliased cells, type 2 Sum of Squares was applied after removing the interaction effects in the model. Two by two effect comparisons were performed either with the contrast function of the contrast package in case of non-nested balanced design, or with the emmeans function of the emmeans package otherwise. Unequal variance t-test (Welch test) was used in bivariate designs. Statistical significance was set to $P \leq 0.05$. In each figure, type I error was controlled by correcting

the *P* values according to the Benjamini & Hochberg method ("BH" option in the p.adjust() function of R). The results of all statistical analyses are detailed in Table S1.

Supplemental references

1. Beutier H, Hechler B, Godon O, Wang Y, Gillis CM, de Chaisemartin L, et al. Platelets expressing IgG receptor FcgammaRIIA/CD32A determine the severity of experimental anaphylaxis. *Sci Immunol.* 2018;3(22).
2. Valenzuela DM, Murphy AJ, Frendewey D, Gale NW, Economides AN, Auerbach W, et al. High-throughput engineering of the mouse genome coupled with high-resolution expression analysis. *Nat Biotechnol.* 2003;21(6):652-9.
3. Dombrowicz D, Brini AT, Flamand V, Hicks E, Snouwaert JN, Kinet JP, et al. Anaphylaxis mediated through a humanized high affinity IgE receptor. *J Immunol.* 1996;157(4):1645-51.
4. Bruhns P, Iannascoli B, England P, Mancardi DA, Fernandez N, Jorieux S, et al. Specificity and affinity of human Fcgamma receptors and their polymorphic variants for human IgG subclasses. *Blood.* 2009;113(16):3716-25.
5. Jakus Z, Nemeth T, Verbeek JS, and Mocsai A. Critical but overlapping role of FcgammaRIII and FcgammaRIV in activation of murine neutrophils by immobilized immune complexes. *J Immunol.* 2008;180(1):618-29.
6. Gross S, Gammon ST, Moss BL, Rauch D, Harding J, Heinecke JW, et al. Bioluminescence imaging of myeloperoxidase activity in vivo. *Nat Med.* 2009;15(4):455-61.
7. Reber LL, Gillis CM, Starkl P, Jonsson F, Sibilano R, Marichal T, et al. Neutrophil myeloperoxidase diminishes the toxic effects and mortality induced by lipopolysaccharide. *J Exp Med.* 2017;214(5):1249-58.
8. Tiller T, Meffre E, Yurasov S, Tsuiji M, Nussenzweig MC, and Wardemann H. Efficient generation of monoclonal antibodies from single human B cells by single cell RT-PCR and expression vector cloning. *J Immunol Methods.* 2008;329(1-2):112-24.
9. Gaudenzio N, Sibilano R, Marichal T, Starkl P, Reber LL, Cenac N, et al. Different activation signals induce distinct mast cell degranulation strategies. *J Clin Invest.* 2016;126(10):3981-98.
10. Team RC. R: A language and environment for statistical computing. *R Foundation for Statistical Computing, Vienna, Austria.* 2018.

Supplemental figures and legends

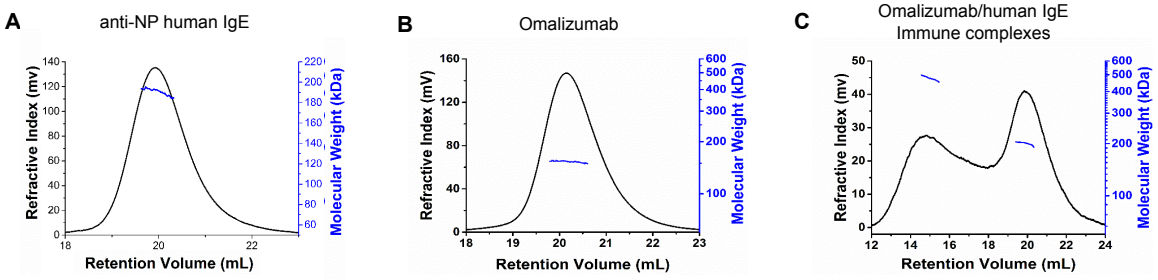

Figure S1. Size exclusion chromatography coupled to static light scattering (SEC-SLS) profiles for human IgE and Omalizumab alone, and for the complex in solution. Anti-NP human IgE (**A**), Omalizumab (**B**) and human IgE/Omalizumab immune complexes (ICs) (**C**) were run through a gel filtration column with a constant flow at 0.3 mL/min. ICs were formed by incubating human IgE and Omalizumab at a 1:2 mass ratio for 1 h at room temperature.

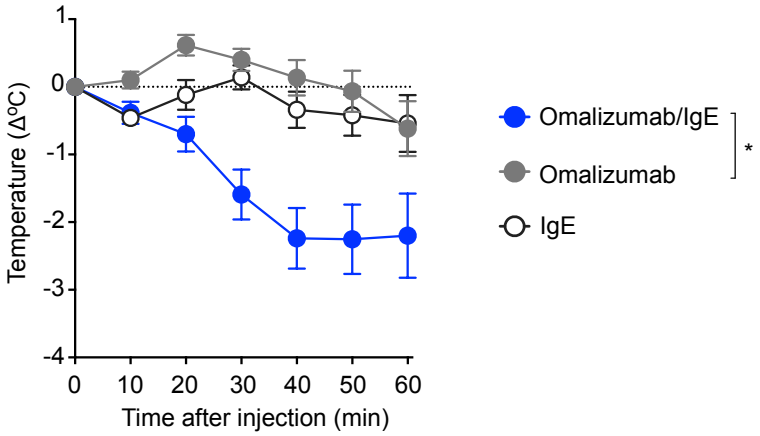

Figure S2. Injection of Omalizumab/IgE ICs triggers passive systemic anaphylaxis in hFcγR^{KI} mice, but not injection of IgE or Omalizumab alone. Changes in body temperature (Δ°C [mean ± SEM]) after intravenous injection of pre-formed Omalizumab/IgE ICs (*n*=13) or anti-NP human IgE (*n*=5) or Omalizumab (*n*=6) alone into hFcγR^{KI} mice. Data are pooled from two (IgE and Omalizumab alone) or three (Omalizumab/IgE ICs) independent experiments. *, $P < 0.05$; using a contrast linear model. Disclosure: data from Omalizumab/IgE treated hFcγR^{KI} mice is the same as presented in Figure 2C. For further details on the statistical analysis, please refer to Table S1.

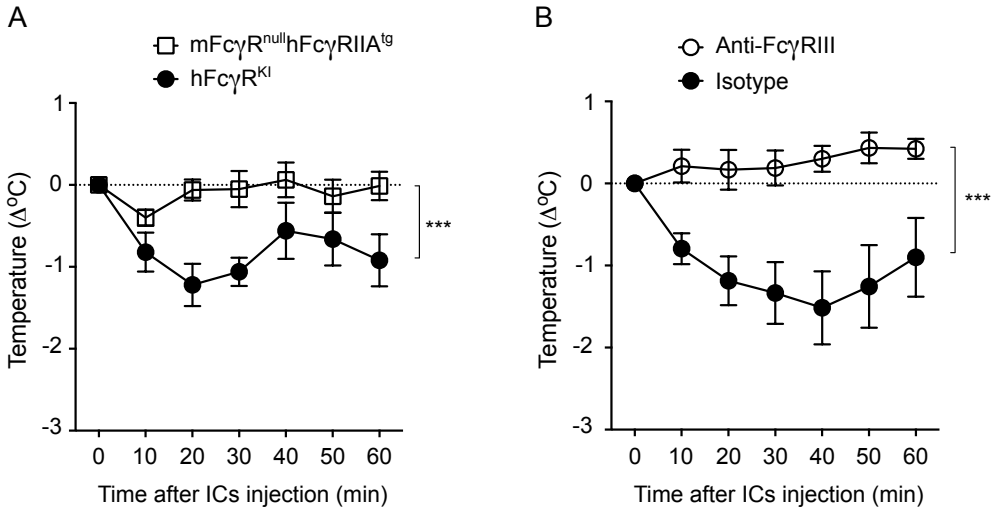

Figure S3. Assessment of the potential role of hFcγRIIA and hFcγRIII in Omalizumab/IgE ICs-induced anaphylaxis. A. Changes in body temperature (Δ°C [mean ± SEM]) after intravenous injection of pre-formed Omalizumab/IgE ICs into hFcγR^{KI} mice (n=6) or mFcγR^{null}hFcγRIIA^{Tg} (n=8). **B.** Changes in body temperature (Δ°C [mean ± SEM]) after intravenous injection of pre-formed Omalizumab/IgE ICs into hFcγR^{KI} mice pre-treated with an anti-hFcγRIII antibody (3G8) (n=8) or an isotype control antibody (n=10). Data in **A** & **B** are pooled from two independent experiments. ***, $P <$ 0.001 using a contrast linear model. For further details on the statistical analysis, please refer to Table S1.

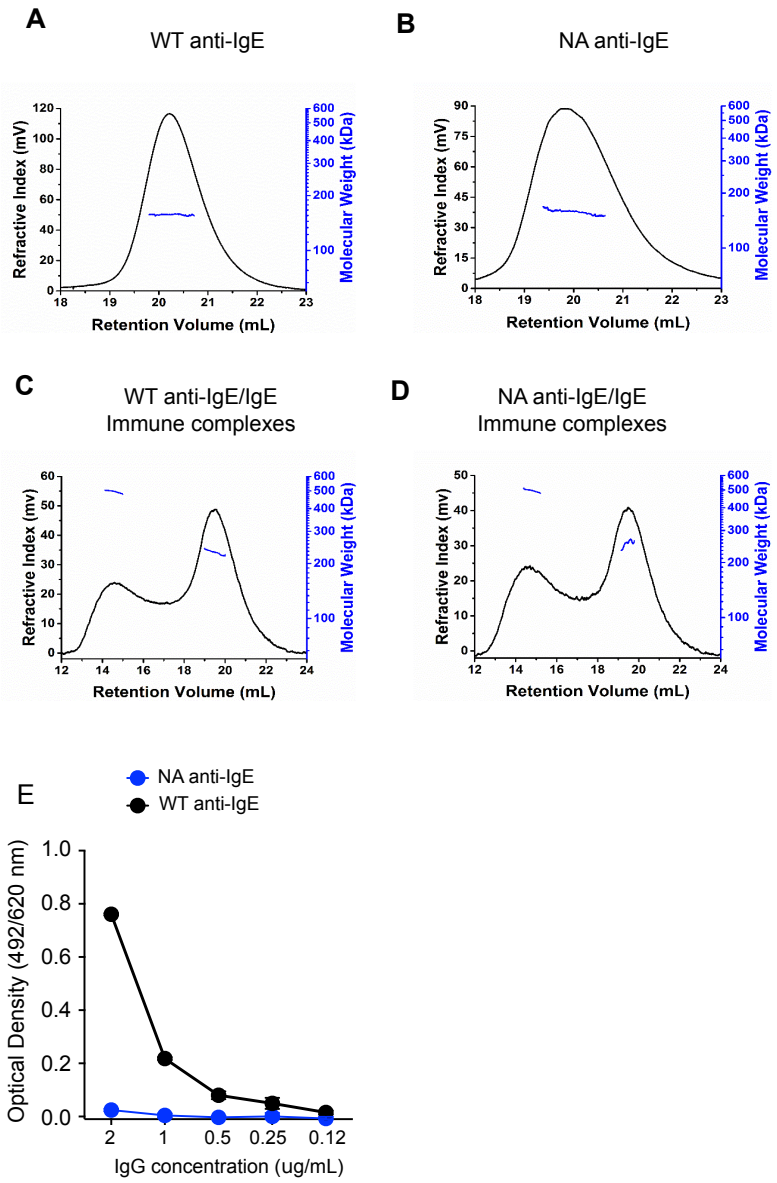

Figure S4. Size exclusion chromatography coupled to static light scattering (SEC-SLS) profiles for WT and NA anti-IgE alone, and in complex with human IgE, and binding of WT or NA anti-IgE to human complement component C1q. (A-D) WT anti-IgE or NA anti-IgE alone (**A** and **B**) or in complex with anti-NP IgE (**C** and **D**) were run through a gel filtration column with a constant flow at 0.3 mL/min. ICs were formed by incubating IgE and anti-IgE mAbs at a 1:2 mass ratio for 1 h at room temperature. (**E**) Binding of WT and NA anti-IgE to human C1q assessed by ELISA. Results in **E** show means ± SD from one out of 2 independent experiments (total of *n=4* replicates).

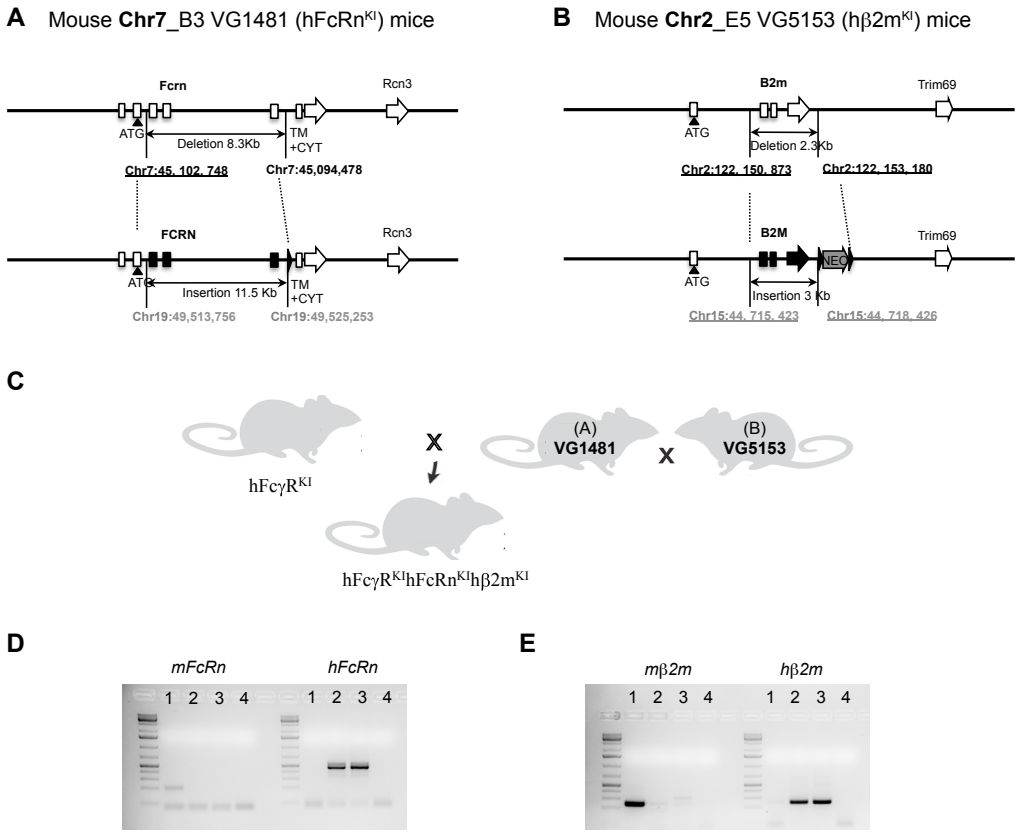

Figure S5. Generation of hFcRn^{KI} and hβ2m^{KI} mice. (**A** and **B**) Humanization of the (**A**) mouse Fcrn gene and (**B**) b2m gene. Representations are not drawn to scale. Coordinates are based on mouse (GRCm38.p4) and human (GRCh38.p7) genomic assemblies: mouse genes are in empty rectangles, genomic coordinates are in black; human genes are in solid rectangles, genomic coordinates are in grey; black triangles represent Loxp site. (**C**) Breeding scheme to obtain hFcγR^{KI}hFcRn^{KI}hβ2m^{KI} mice. (**D** and **E**) RT-PCR analysis of mFcRn and hFcRn (**D**) and mβ2m and hβ2m (**E**). 1: splenocytes from hFcγR^{KI} mice; 2: splenocytes from hFcγR^{KI}hFcRn^{KI}hβ2m^{KI} mice; 3: Human PBMC; 4: negative control.

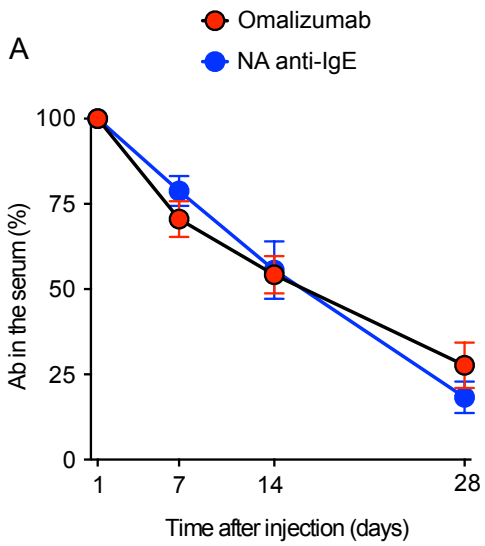

Figure S6. Comparison of the *in vivo* half-life of Omalizumab and the NA anti-IgE mAbs. 100 µg of Omalizumab or NA anti-IgE was injected intraperitoneally (i.p.) into hFcγR^{KI}hFcRn^{KI}hβ2m^{KI} mice, and serum was collected at different time-points. Levels of anti-IgE mAbs were measured by ELISA. Data are indicated as means ± SEM pooled from two independent experiments (n=7-8/group). Differences between both groups were not statistically significant ($P > 0.05$ by ANOVA).

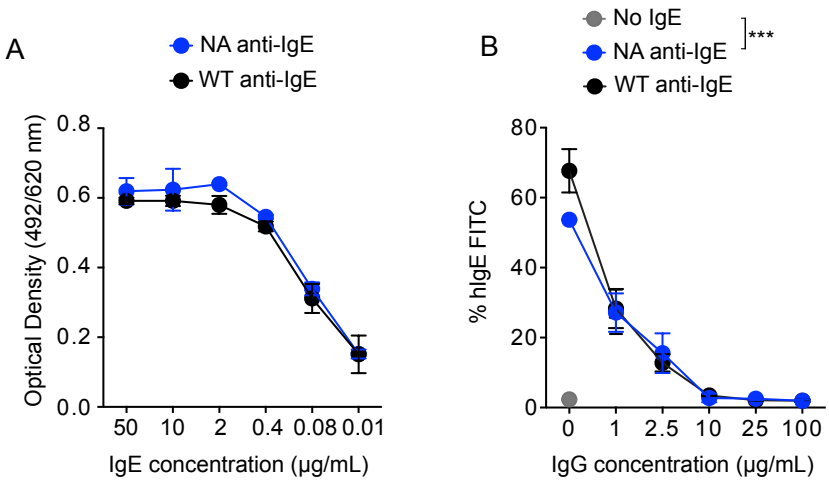

Figure S7. Characterization of recombinant WT anti-IgE and NA anti-IgE mAbs. (**A**) Binding of WT and NA anti-IgE to IgE assessed by ELISA. Results show means ± SD from data pooled from two independent experiments. (**B**) Human mast cells (hMCs) expressing the high-affinity IgE receptor FcεRI were preincubated with WT or NA anti-IgE at the indicated concentration. FITC-labeled IgE were added immediately after and hMCs were incubated for 16 hours before levels of FITC-IgE bound to hMCs was assessed by flow cytometry. Data show means ± SD from one representative of three independent experiments.

	Comparison	Alternative hypothesis	Sample size	Test	*P*-value	Adjusted p-value
1B	Omalizumab and IgG1.K322A	Mean effect	n = 20, n = 20	Anova, df_{num} = 1, df_{denom} = 20	< 2e-16	NA
1C	Medium and IgE	effect difference	n = 14, n = 14 | df = 10.6, df = 10.6	Contrast test in linear model	0.005	0.005
	Mediuma and Omalizumab-IgE	effect difference	n = 14, n = 14 | df = 10.6, df = 10.6	Contrast test in linear model	5e-11	2e-10
	IgE and Omalizumab-IgE	effect difference	n = 14, n = 14 | df = 10.6, df = 10.6	Contrast test in linear model	2e-7	3e-7
1D	Medium and IgE	effect difference	n = 14, n = 14 | df = 6.2, df = 6.2	Contrast test in linear model	1e-8	1e-8
	Medium and Omalizumab-IgE	effect difference	n = 14, n = 14 | df = 6.2, df = 6.2	Contrast test in linear model	4e-15	5e-15
	IgE and Omalizumab-IgE	effect difference	n = 14, n = 14 | df = 6.2, df = 6.2	Contrast test in linear model	4e-15	5e-15
1E	Medium and IgE	effect difference	n = 14, n = 14 | df = 5.8, df = 5.8	Contrast test in linear model	0.10	0.10
	Medium and Omalizumab-IgE	effect difference	n = 14, n = 14 | df = 5.8, df = 5.8	Contrast test in linear model	2e-10	6e-10
	IgE and Omalizumab-IgE	effect difference	n = 14, n = 14 | df = 5.8, df = 5.8	Contrast test in linear model	3e-8	5e-8
1F	Medium and ICs in hFcgRKI	mean difference	n = 5, n = 5	Welch test	0.003	0.01
	Medium and ICs in FcgRnull	mean difference	n = 4, n = 4	Welch test	0.89	0.89
	hFcgRKI and FcgRnull in medium	mean difference	n = 5, n = 4	Welch test	0.68	0.89
	hFcgRKI and FcgRnull in IC	mean difference	n = 5, n = 4	Welch test	0.02	0.04
2B	Saline and IgE in hFcgRKI	effect difference	n = 9, n = 9 | df = 22.2, df = 22.2	Contrast test in linear model	0.48	0.58
	Saline and Omalizumab in hFcgRKI	effect difference	n = 9, n = 9 | df = 22.2, df = 22.2	Contrast test in linear model	0.35	0.52
	Saline and Omalizumab-IgE in hFcgRKI	effect difference	n = 9, n = 9 | df = 22.2, df = 22.2	Contrast test in linear model	4e-9	3e-8
	IgE and Omalizumab in hFcgRKI	effect difference	n = 9, n = 9 | df = 22.2, df = 22.2	Contrast test in linear model	0.99	0.99
	IgE and Omalizumab-IgE in hFcgRKI	effect difference	n = 9, n = 9 | df = 22.2, df = 22.2	Contrast test in linear model	6e-8	2e-7
	Omalizumab and Omalizumab-IgE in hFcgRKI	effect difference	n = 9, n = 9 | df = 22.2, df = 22.2	Contrast test in linear model	9e-8	2e-7
	Saline and IgE in FcgRnull	effect difference	n = 8, n = 8 | df = 14.6, df = 14.6	Contrast test in linear model	0.01	0.04
	Saline and Omalizumab in FcgRnull	effect difference	n = 8, n = 8 | df = 14.6, df = 14.6	Contrast test in linear model	0.07	0.11
	Saline and Omalizumab-IgE in FcgRnull	effect difference	n = 8, n = 8 | df = 14.6, df = 14.6	Contrast test in linear model	1e-4	8e-4
	IgE and Omalizumab in FcgRnull	effect difference	n = 8, n = 8 | df = 14.6, df = 14.6	Contrast test in linear model	0.85	0.85
	IgE and Omalizumab-IgE in FcgRnull	effect difference	n = 8, n = 8 | df = 14.6, df = 14.6	Contrast test in linear model	0.16	0.19
	Omalizumab and Omalizumab-IgE in FcgRnull	effect difference	n = 8, n = 8 | df = 14.6, df = 14.6	Contrast test in linear model	0.03	0.07
2C	hFcgRKI - Omalizumab_IgE and FcgRnull - Omalizumab_IgE	effect difference	n = 91, n = 63 | df = 29, df = 29	Contrast test in linear model	0,003	0,01
2D	hFcgRKI and hFcgRKIC1q-/-	Mean effect	n = 63, n = 56	Anova, df_{Chi2} = 1	5e-4	NA
3B	Medium and WT-IgE	effect difference	n = 14, n = 14 | df = 7.2, df = 7.2	Contrast test in linear model	1e-13	3e-13
	Medium and NA-IgE	effect difference	n = 14, n = 14 | df = 7.2, df = 7.2	Contrast test in linear model	4e-6	4e-6
	WT-IgE and NA-IgE	effect difference	n = 14, n = 14 | df = 7.2, df = 7.2	Contrast test in linear model	7e-8	1e-7
3C	Medium and WT-IgE	effect difference	n = 14, n = 14 | df = 5.7, df = 5.7	Contrast test in linear model	4e-15	1e-14
	Medium and NA-IgE	effect difference	n = 14, n = 14 | df = 5.7, df = 5.7	Contrast test in linear model	8e-11	8e-11
	WT-IgE and NA-IgE	effect difference	n = 14, n = 14 | df = 5.7, df = 5.7	Contrast test in linear model	7e-15	1e-14
3D	Medium and WT-IgE	effect difference	n = 14, n = 14 | df = 5.3, df = 5.3	Contrast test in linear model	2e-10	6e-10
	Medium and NA-IgE	effect difference	n = 14, n = 14 | df = 5.3, df = 5.3	Contrast test in linear model	0.05	0.05
	WT-IgE and NA-IgE	effect difference	n = 14, n = 14 | df = 5.3, df = 5.3	Contrast test in linear model	9e-8	1e-7
3E	WT and NA	Mean effect	n = 62, n = 62	Anova, df_{Chi2} = 1	0.58	NA

	Comparison	Alternative hypothesis	Sample size	Test	*P*-value	Adjusted p-value
4A	hFceRI- PBS and hFceRI.Tg PBS	effect difference	n = 28, n = 28 | df = 14.3, df = 14.3	Contrast test in linear model	2e-4	4e-4
	hFceRI- PBS and hFceRI.Tg Omalizumab	effect difference	n = 28, n = 35 | df = 14.3, df = 13.9	Contrast test in linear model	0.97	1
	hFceRI- PBS and hFceRI.Tg NA anti-IgE	effect difference	n = 28, n = 35 | df = 14.3, df = 13.9	Contrast test in linear model	0.98	1
	hFceRI.Tg PBS and hFceRI.Tg Omalizumab	effect difference	n = 28, n = 35 | df = 14.3, df = 13.9	Contrast test in linear model	6e-5	2e-4
	hFceRI.Tg PBS and hFceRI.Tg NA anti-IgE	effect difference	n = 28, n = 35 | df = 14.3, df = 13.9	Contrast test in linear model	6e-5	2e-4
	hFceRI.Tg Omalizumab and hFceRI.Tg NA anti-IgE	effect difference	n = 35, n = 35 | df = 13.9, df = 13.9	Contrast test in linear model	1	1
4C	Saline and IgE in hFcgRKI	effect difference	n = 28, n = 35 | df = 35.3, df = 35.3	Contrast test in linear model	0.19	0.22
	Saline and Omalizumab in hFcgRKI	effect difference	n = 28, n = 35 | df = 35.3, df = 35.3	Contrast test in linear model	0.001	0.003
	Saline and Omalizumab-IgE in hFcgRKI	effect difference	n = 28, n = 35 | df = 35.3, df = 35.3	Contrast test in linear model	2e-5	1e-4
	IgE and Omalizumab in hFcgRKI	effect difference	n = 28, n = 35 | df = 35.3, df = 35.3	Contrast test in linear model	0.14	0.20
	IgE and Omalizumab-IgE in hFcgRKI	effect difference	n = 28, n = 35 | df = 35.3, df = 35.3	Contrast test in linear model	0.005	0.01
	Omalizumab and Omalizumab-IgE in hFcgRKI	effect difference	n = 28, n = 35 | df = 35.3, df = 35.3	Contrast test in linear model	0.48	0.48
	Saline and IgE in FcgRnull	effect difference	n = 11, n = 11 | df = 24.8, df = 24.8	Contrast test in linear model	0.005	0.02
	Saline and Omalizumab in FcgRnull	effect difference	n = 11, n = 11 | df = 24.8, df = 24.8	Contrast test in linear model	0.004	0.02
	Saline and Omalizumab-IgE in FcgRnull	effect difference	n = 11, n = 11 | df = 24.8, df = 24.8	Contrast test in linear model	0.03	0.05
	IgE and Omalizumab in FcgRnull	effect difference	n = 11, n = 11 | df = 24.8, df = 24.8	Contrast test in linear model	1	1
	IgE and Omalizumab-IgE in FcgRnull	effect difference	n = 11, n = 11 | df = 24.8, df = 24.8	Contrast test in linear model	0.91	1
	Omalizumab and Omalizumab-IgE in FcgRnull	effect difference	n = 11, n = 11 | df = 24.8, df = 24.8	Contrast test in linear model	0.85	1
4D	Omalizumab and NA anti-IgE	Mean effect	n = 70, n = 77	Anova, df_{Chi2} = 1	5e-7	NA
S2	hFcgRKI - IgE and FcgRnull - Omalizumab_IgE	effect difference	n = 35, n = 63 | df = 29, df = 29	Contrast test in linear model	0,93	1
	hFcgRKI - Omalizumab and FcgRnull - Omalizumab_IgE	effect difference	n = 42, n = 91 | df = 29, df = 29	Contrast test in linear model	1	1
	hFcgRKI - Omalizumab and hFcgRKI - IgE	effect difference	n = 42, n = 35 | df = 29, df = 29	Contrast test in linear model	0,91	1
	hFcgRKI - Omalizumab_IgE and hFcgRKI - IgE	effect difference	n = 91, n = 35 | df = 29, df = 29	Contrast test in linear model	0,07	0,13
	hFcgRKI - Omalizumab_IgE and hFcgRKI - Omalizumab	effect difference	n = 91, n = 42 | df = 29, df = 29	Contrast test in linear model	0,006	0,02
S3A	hFcgRKI and FcgRnullI-hFcgRIIA.Tg	Mean effect	n = 35, n = 56	Anova, df_{Chi2} = 1	0.001	NA
S3B	Anti-FcgRIII and Isotype	Mean effect	n = 63, n = 70	Anova, df_{Chi2} = 1	1e-5	NA
S5B	no.IgE and WT.anti.IgE in Conc 0	mean difference	n = 3, n = 2	Welch test	0.06	0.12
	no.IgE and NA.anti.IgE in Conc 0	mean difference	n = 3, n = 2	Welch test	4e-6	2e-5
	WT.anti.IgE and NA.anti.IgE in Conc 0	mean difference	n = 2, n = 2	Welch test	0.26	0.35
S7A	WT.anti-IgE and NA.anti-IgE	Mean effect	n = 12, n = 12	Anova, df_{num} = 1, df_{denom} = 5	0.08	NA
S7B	WT.anti-IgE curve and NA.anti-IgE curve	Mean effect	n = 12, n = 12	Anova, df_{num} = 1, df_{denom} = 25	0.62	0.62

Table S1. Statistical analyses. n, sample size for each class tested, respectively; df, degree of freedom; adjusted p values from the same panel, according to Benjamini & Hochberg.